Development of jet-gun and fluidization enhanced pile installation tools

Ben Arntz [i)], Leo van der Bijl [ii)], Govert Meijer [iii)], Dirk Luger [iv)]

i) Founder & Director, GBM Works BV, Atoomweg 7-9, 3542 AA, Utrecht, The Netherlands.

ii) Product Development Engineer, GBM Works BV, Atoomweg 7-9, 3542 AA, Utrecht, The Netherlands.

iii) Director, GBM Works BV, Atoomweg 7-9, 3542 AA, Utrecht, The Netherlands.

iv) Geotechnical Consultant, Deltares, Boussinesqweg 1, 2629 HV Delft, The Netherlands

ABSTRACT

Installation of large monopiles by impact hammering is becoming increasingly difficult. Partially because increasing pile sizes push the limits of the capacity of hammers and anvils; partially because restrictions regarding noise emission restrict the use of these hammers. Because of this there are many initiatives for developing alternative methods and tools for installation of monopiles. One concept that stands out is based on the temporary reduction of soil resistance on the inside of a monopile, using a water jetting gun technique, combined with vibro driving.
Water jetting and soil fluidisation have been around since long, but this largely grew from empirical practice while the combination of theoretical knowledge with large scale offshore applications has been quite limited. Main research questions concerned the prediction of the required operational parameters for the jetgun (like pressure, flow rate, nozzle configuration, etc.) and the vibro tool (frequency, amplitude, etc.) for successful installation, as a function of soil and monopile parameters. For a pile installation to be successful it is essential that the soil integrity under the pile tip and next to the pile is preserved while the soil inside the pile is fluidised.
This paper presents an overview of the desk research, scaled lab tests and scaled field tests that have been performed during the development of a new installation method, based on a vibro tool at the top of the monopile, in combination with a retrievable jetgun near the toe of the pile. The paper focusses on jetting and fluidisation installation aspects in a largely non-cohesive (i.e. a sandy, silty) seabed.

Keywords: research, lab testing, field testing, jetting, fluidisation, monopile installation

1 INTRODUCTION

As stated in the abstract, there is a great need to find better ways to install large monopiles: While vibro-installation offers great advantages over impact driving in terms of generated noise, the drawback of vibro-blocks is that these meet pile refusal conditions too early. The new development, of which a part of the concept R&D is described in this paper enhances the pile installation speed as well as the installable depth of the vibro-installation as was known till now. The development goes through a series of stages, ever reaching to higher TRL levels in a series of JIP development programmes, comprising the now completed SIMPLE-I, which is the basis for this paper and the ongoing SIMPLE-II and SIMOX projects.

While in the future a tool is envisaged whereby not only the soil inside the pile wall is fluidised but also the driving vibrations are led into the pile in the vicinity of the pile tip to install faster and generate even less noise, the current approach is more robust and can be introduced to the offshore practice sooner since more parts have a proven track record: The current version is one where the vibration is applied at the top of the pile using proven technology and where a jet-ring, positioned inside the pile near its tip, has two vital functions. First the jet-ring must provide a flow rate that is sufficient to fluidise the soil at the inside pile wall and destroy the interface friction that resists the pile installation, and second the jet ring must create room for its own downward penetration, both in sand and occasional clayey layers.

The first function requires fluidisation, and the second function requires a mix of cutting, erosion and fluidisation. Cutting, erosion and fluidisation, in that order, require high to medium to low water pressures and low to medium to high water flows respectively.

2 JETTING PROCESS

The jets are placed in a ring near the pile tip at the inside of the pile in such a way that they will not reach the level of the pile tip itself. Thanks to their position and orientation they cover the complete circumference of the soil under the jet ring and generate a vortex flow pattern that enhances flow along the inside wall of the pile rather than the pile axis. This way the jets erode and cut soil that poses a resistance to the lowering of the jet ring itself while supplying sufficient water to create a fluidised zone along the inside of the pile. While for the overall R&D project jets have been tested in relation to their ability to cut into medium strong and very strong clays the focus for this first tool was on the performance in sand and the contribution of the jet flow to the fluidisation along the pile wall.

3 FLUIDISATION PROCESS

The flow that is produced by the jetgun creates an upward gradient of groundwater pressure in the soil column inside the pile. For a certain uniform upward water flow through the soil column the sand grains start to be carried by the water rather than by their neighbouring grains and the sand body loses its capacity to transfer shear stresses. This flow occurs at the "critical gradient" i_c (-) and is equal to:

$$i_c = (\frac{\rho_s}{\rho_f} - 1)(1 - n) \quad (1)$$

Where ρ_s and ρ_f are the grain and fluid densities and n is the porosity of the sand. For relatively uniform flow conditions occurring at gradients below and slightly above i_c the flow velocity q (m/s) follows with the permeability of the sand body, k (m/s), according to Darcy's Law:

$$q = k\, i_c \quad (2)$$

The permeability of the sand bed primarily depends on its porosity and the grain size distribution. For the development of the fluidisation technique a series of laboratory tests was performed to investigate the homogeneity of the flow, the ability to fluidise the whole sand column by injecting water over the complete base area but also by just injecting water along the inner edge of the pile, the required flows at various bed expansion levels, the time over which the column would settle and consolidate after stopping water injection as well as the time required to re-fluidise and to attain a steady state fluidisation again.

4 LAB SCALE FLUIDISATION TESTS

The upward groundwater flow decreases the interparticle (effective) stresses leading to a small expansion of the bed, an increase of the porosity n and with that an increase of the permeability of the sand body. At higher flow rates the sand column expands further, the grains become more dispersed, and the permeability can be associated with the hindered settling velocity of the sand particles. This process was investigated at three increasing lab scales in columns with height / diameters of 1.0 m / 0.15 m, 2.0 m / 0.3 m and 4.2 m / 0.6 m respectively. The field tests that are described in section 5 involved again a doubling in diameter. In the laboratory tests, the investigation addressed, apart from the fluidisation itself, also under which circumstances a vibratory tool could be lowered and raised through the fluidised sand column and how, after stopping the flow and allowing the sand to sediment and consolidate, the sand could be fluidised again.

4.1 Test set-up

The last tests series was performed in the largest 4.2 m high, 0.6 m diameter column. A pump and recirculation system delivers an adjustable flow through the sand column. Fig. 1 shows the schematic set-up in the lab.

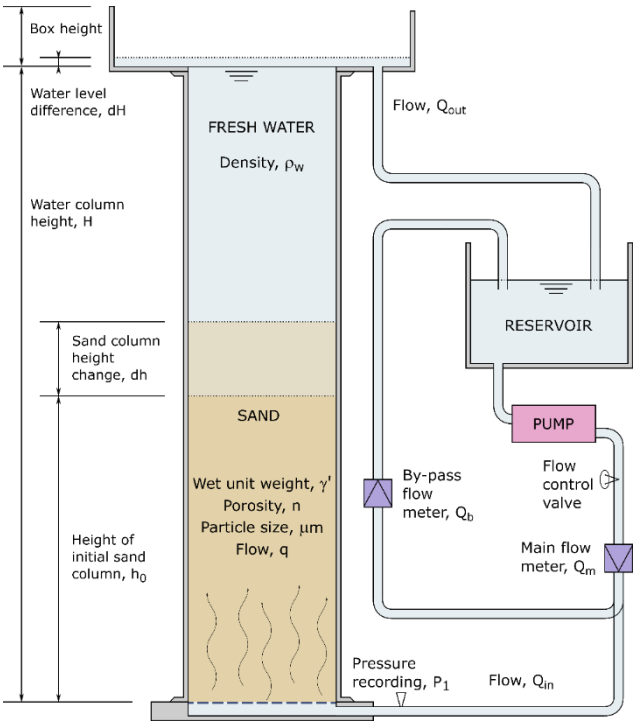

Fig. 1. Set-up of the test system with the various test parameters.

The system was driven by a 60m^3/hour @ 400 kPa capacity frequency-controlled pump. Monitoring took place using pressure transducers and flow meters as indicated in Fig. 1, which were logged with a 19 Hz sampling rate. A Canon digital camera 1100D (DSRL) connected to a PC was used to semi-continuously

(0.2 Hz) record the test. From the camera stills, the change in bed height was derived using specially developed scripts. As back-up, the bed height was also recorded manually. Fig. 2 gives an impression of the bottom half of the column in an initial (height 1.365 m) and expanded (1.940 m) state.

Fig. 2. 0.6m diameter column with initial sand bed (left) and expanded sand bed (right) as recorded during test 04.

4.2 Testing program

While sands with D_{50} ranging from 150 to 912 μm were used in the smaller scale tests, the digitally recorded tests in the 0.6m column focussed on an intermediate sand with properties as shown in Table 1.

Table 1. Properties of sand tested in 0.6 m diameter column.

Description	Unit	Sand B
Type of sand		Baskarp, silica
D_{10}	[μm]	153
D_{50}	[μm]	222
D_{60}	[μm]	238
e_{min}	[-]	0.543
e_{max}	[-]	0.848

Tests were performed in the large columns, with different sand densities, column heights and flow regimes, as shown in Table 2.

Table 2. Testing program on uniform sand columns.

Test	Dr [%]	H0 [m]	Imposed flow [l/min] (see note*)
1	51	1.470	0 / 40 \ 0 / 40 ↓ 0
2	37	1.514	0 // 36 \\ 0 // 36 ↓ 0
3	52	1.465	2 x [0 ↑ 24 ↑ 48 ↓ 24 ↓ 0] ↑ 48 ↓ 0
4	87	1.365	0 / 40 \ 0 / 40 ↓ 0
5	90	1.357	0 ↑ 12 ↑ 24 ↑ 32 ↓ 0
6	91	1.354	0 ↑ 24 ↑ 48 ↓ 0

(*): /,\ indicate 8 l/min steps, //,\\ indicate 12 l/min steps; ↑,↓ indicate abrupt flow changes from one value to the other.

The flow rate was imposed in a swift change from one rate to the other, after which the development of a steady state would gradually develop before increasing or decreasing to the next flow rate. In addition to these tests also tests with layered soil columns were executed, to observe the effect of layering on the fluidisation, segregation and mixing of the sand types.

4.3 Test results

Fig. 3 and 4 below show a characteristic response of the sand column as a function of the changing flow regime.

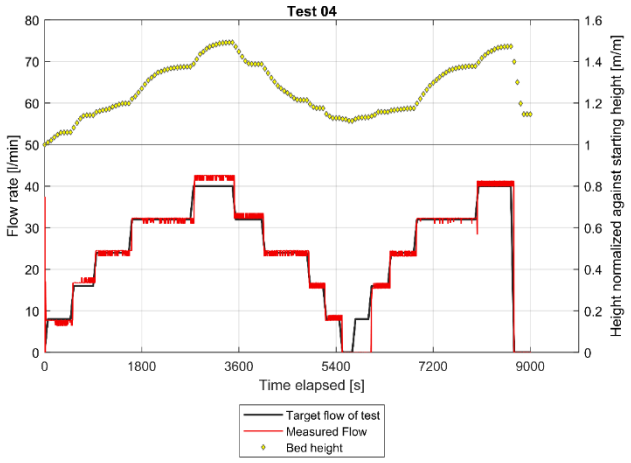

Fig. 3. Bed height and flow rate during test 4 on sand B.

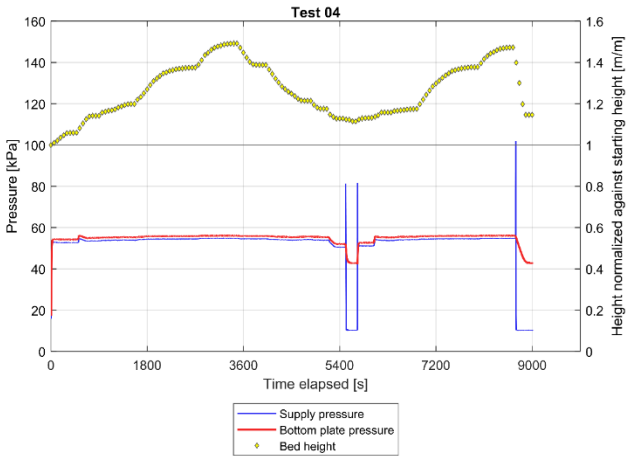

Fig. 4. Bed height and bottom plate pore pressure for test 4.

Studying the results in more detail one finds that only after t = 1080 s the sand is first fluidised and expanded beyond 0% relative density at a normalised bed height of 1.16 m/m. For this sand the transition between solid and fluid states occurs between flow rates of 16 and 24 l/min (nett flow velocities between q = 0.9 and 1.4 mm/s). The small pressure jumps at t = 600 s and t = 6180 s exceed temporarily the static weight of sand and water since during those phases the sand is not fully liquefied, and part of the excess pressure can be taken by shear along the inner wall of the column. One sees that the pressure at the base-filter is hardly changing with the flow rate. This makes sense since the effective stresses in the liquefied sand are virtually zero and the total stress represents the weight of the water column plus

suspended sand grains. When the flow rate is increased it takes time for the bed to adjust to its new equilibrium. From the rate of inflow at the base (q_{in} [m/s]) and the groundwater head gradient (i [m/m]) over the height of the sand column an apparent permeability k_{app} [m/s] can be derived using eq. (2). The term apparent permeability is used, since while the column expansion or contraction is going on, the flow at the top of the column differs from the flow at the base and while we know the average void ratio there will be a non-uniform void ratio during the unsteady phase. The average void ratio and the apparent permeability k_{app} in test 4 are shown as function of time in Fig. 5. For reference the maximum void ratio of the sand is indicated by a thick line at e = 0.848.

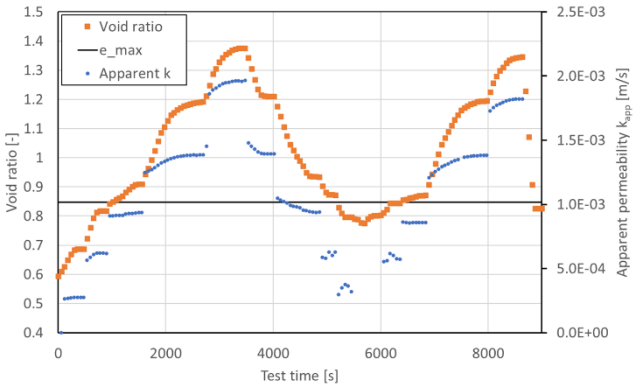

Fig. 5. Average void ratio and apparent permeability in test 4.

Fig. 5 also shows that after stepwise reducing the flow (around t = 5600 s) the relative density of the column reached a value around D_r = 24 %. After an abrupt stop of the flow the sand settled into a very loose state with a relative density as low as D_r = 7 %.

An interesting result follows when for all data points the average void ratio and the apparent permeability are plotted against each other, as shown in Fig. 6. It turns out that even in non-steady states, irrespective of being in an expanding or a contracting phase of the test the measured inflow is a unique function of the average void ratio and apparent permeability.

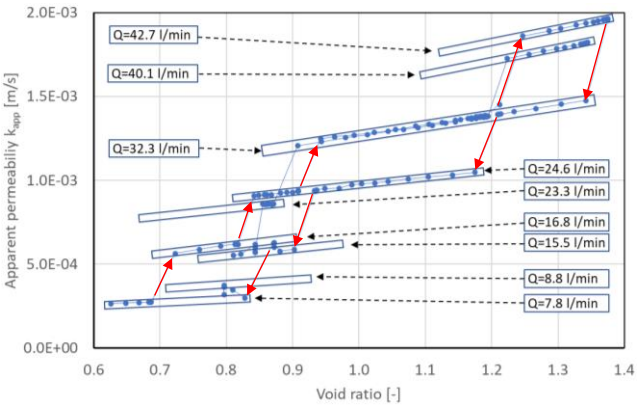

Fig. 6. Inflow Q as a unique function of e_{avg} and k_{app}. Red arrows indicate path of first increase and decrease cycle of Q.

Not only do these measurements provide insight in the change of sedimentation rates under upward (counteracting) or downward (enhancing) flows, but these findings also form the basis of ongoing research into the migration of solids and changes in solids concentration distributions within the sand column from one steady state to the other. Especially for the theoretical analysis of the scale-up the time-dependent response on changes in the flow rates are relevant since the process involves a mix between sedimentation (for void ratios higher than e_{max}) and consolidation processes (for void ratios smaller than e_{max}). How these two contribute is important, since the sedimentation time is essentially linear with the pile length, while the consolidation (pore pressure dissipation) time is proportional with the square of the pile length.

5 SCALE-UP AND FIELD TESTING

Field testing took place at the Maasvlakte near Rotterdam, at a site that was used for earlier pile load tests for the Rotterdam Port Authorities and was made available for the jet-supported pile installation tests.

Fig. 7. Test site with 800 m^3 jet water reservoir at the right.

To differentiate between pile vibro-installation without and with jetgun support special attention was paid to the site and the selection of locations where different methods could be compared with a minimum of differences between the soil conditions.

5.1 Local test location optimisation

The site was extensively investigated by a cone penetration testing (CPT) campaign. In addition to 13 CPTs that were available from earlier pile load tests at the site 53 extra CPTs were performed at potential test locations to characterise the site, see Fig. 8.

A special approach was developed for the optimal combination of tests at different CPT locations. With the 53 new CPTs 1378 unique CPT pairs were defined. Each CPT was divided into 0.5 m sections and per section the average cone resistance was determined. Between the two CPTs in a pair the absolute differences between all 0.5 m sections were summed.

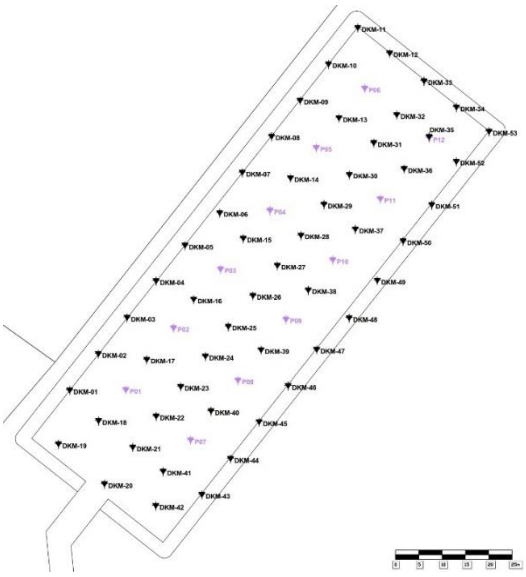

Fig. 8. Test site with CPT locations (scale bar shows 5 m blocks)

The lower the summed value, the more the two CPTs in the pair were similar. The "heat map" in Fig. 9 shows the result where dark blue represents a high correlation within the pair and yellow indicates the worst matches. The blocks on the diagonal show the darkest blue colour since these represent the perfect correlation of a CPT with itself.

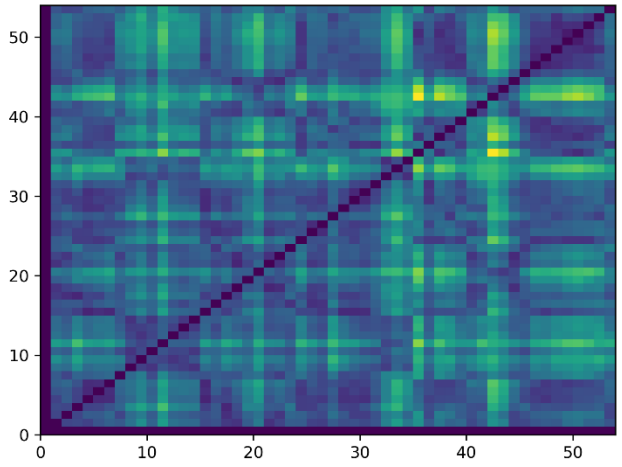

Fig. 9. Heat map used to combine tests at different CPT locations

The CPT groups were divided into three categories and were sharing either low, medium or high cone resistances.

5.2 Test set-up

In total 4 different piles were used. Two smaller piles with a 0.762 m diameter and two larger piles with a 1.220 m diameter. All piles were12 m long. One of the smaller and one of the larger piles was equipped with the GBM Works jetgun system. A Woltman 1000 PDS crane with a PVE 24VM vibro block was mobilised for the installation, together with a 2 m^3/min Kamat plunger pump to drive the jetting system. In this way (for a fixed setting of the vibro-eccentric moment of 9.1 and 12 kgm for the smaller and the larger pile respectively) installation speed and refusal depth (if any) could be compared without the jetgun and with the jetgun operating at different flow rates.

For safety, the pile was vertically supported by the crane during the initial stage of the installation until the pile was sufficiently stable by soil support. During the tests extensive monitoring took place, comprising penetration depth and speed versus time, crane load, pile head acceleration and amplitude together with the power, pressure and frequency readings of the vibro-block. For the jetgun operation also the water pressure, flow rate, and water level in the pile were recorded. Comparison of flowrate and water volume in the pile was also used to confirm that no piping (excessive water loss) past the pile tip and along the outside of the pile did occur.

5.3 Test results – ease of installation

Piles were installed without jetgun and with varying jetgun flow rates to find optimal settings.

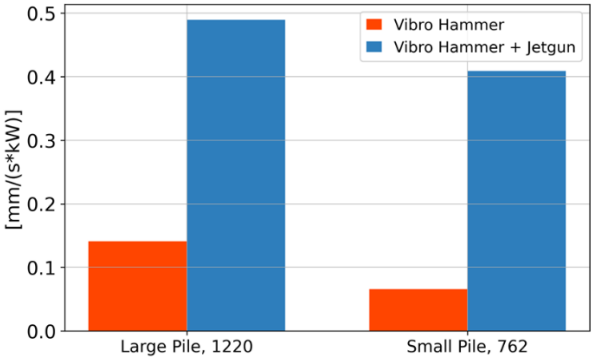

Fig. 10. Penetration rate divided by power

For the larger pile, the penetration efficiency (here defined as speed over power) with operational jetgun increased with a factor between 2.5 and 4.03 with an average around 3.5. For the smaller pile the penetration efficiency with operational jetgun increased with a factor between 3.8 and 10.6 with an average around 6.4.

5.4 Test results – refusal depth

Special tests were performed to compare the maximum achievable penetration depth with and without jetgun operation. For these tests the vibro-block setting was reduced to 6 kgm to increase the likelihood that using only the vibro-block would result in a pile not reaching its full depth. In this way a comparison of refusal depth with and without the jetgun was made possible. Fig. 11 shows the averages for the two pile types.

With the low power vibro-block setting, without jetting, the larger pile stopped already before reaching 2.5 m penetration. With the jetgun supporting the vibro-block the same pile reached 4, 8 and 10 m penetration depth at comparable CPT profiles.

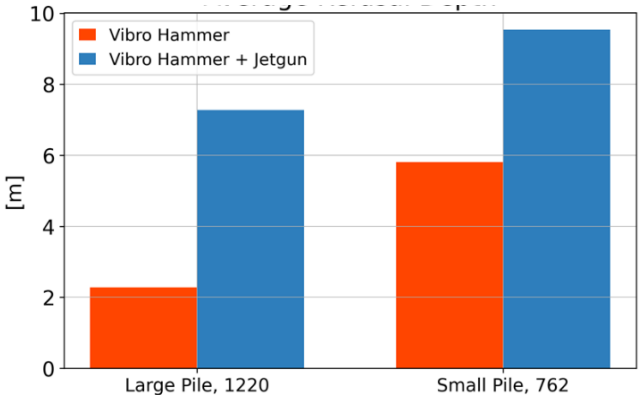

Fig. 11. Average refusal depth with and without jetgun

Using the same vibro-block setting on the smaller pile without jetting two out of three piles met refusal around 4 m penetration and only one pile reached its target penetration depth. With assistance of the jetgun all the small piles reached their target penetration (10 m) at all CPT locations.

5.4 Test results – Dummy vibro-tool retrieval

Since one of the future options is to apply the vibratory energy near the pile tip it was investigated to what extent a (dummy) vibro-tool could be retrieved from the tip of the pile. The case where the sand had settled and locked the tool due to an (unintended) stop of the jetgun flow was of particular interest. Two tests were performed to investigate this aspect, and both proved that the vibro-tool could be retrieved successfully, even after a flow interruption which let the sand solidify and initially locked the vibro-tool. The sedimentation and potential blocking of jetgun nozzles did not present fluidisation of the sand and subsequent retrieval of the dummy vibro-tool from the deep end of the pile.

6 CONCLUSIONS

The following conclusions were drawn from these tests:

The fluidisation of the sand column in the pile can be modelled and gives consistent and repeatable test results which are the basis for an operational fluidisation model.

The use of the jetgun significantly increased the installation efficiency, thus reducing installation time as well as the level and duration of noise load on the marine environment.

The measurements gave no indication whatsoever that the soil outside the pile was compromised by jetgun induced waterflow. The soil outside the pile is governing for its lateral bearing capacity, where the inside soil is of minor important.

Retrieval of tools that are deployed at the deep end of the pile proved to be feasible.

6.1 Further development and verification.

As indicated the development is ongoing within various JIP research programs (a.o. SIMPLE-II and SIMOX).

Within the field-testing scope of this StressWave conference additional test installations and axial test loadings are foreseen. These tests will focus on further jetgun improvements, verification of the sand fluidisation model in-situ and on the effect of the various installation parameters on the vertical bearing capacity.

ACKNOWLEDGEMENTS

The support by the RvO under the “Topsector Energie 2019” subsidy program “Herwinbare Energie” and the assistance from the Rotterdam Port Authorities for making their test site and facilities available for the field tests are thankfully acknowledged.